Molecular Cell, Vol. 9, 163–173, January, 2002, Copyright ©2002 by Cell Press

LTRPC2 Ca^{2+}-Permeable Channel Activated by Changes in Redox Status Confers Susceptibility to Cell Death

Yuji Hara,[1,4] Minoru Wakamori,[2] Masakazu Ishii,[1,5] Emi Maeno,[3,4] Motohiro Nishida,[1] Takashi Yoshida,[1,4] Hisanobu Yamada,[1] Shunichi Shimizu,[6] Emiko Mori,[1] Jun Kudoh,[7] Nobuyoshi Shimizu,[7] Hitoshi Kurose,[8] Yasunobu Okada,[3,4,9] Keiji Imoto,[2,4] and Yasuo Mori[1,4,10]

[1] Center for Integrative Bioscience
[2] Department of Information Physiology
[3] Department of Cell Physiology
National Institute for Physiological Sciences
[4] School of Life Science
The Graduate University for Advanced Studies
Okazaki 444-8585
[5] Department of Clinical Pharmacy
[6] Department of Pathophysiology
School of Pharmaceutical Sciences
Showa University
Tokyo 142-8555
[7] Department of Molecular Biology
Keio University School of Medicine
Tokyo 160-8582
[8] Laboratory of Pharmacology and Toxicology
Graduate School of Pharmaceutical Sciences
University of Tokyo
Tokyo 113-0033
[9] CREST, Japan Science and Technology Corporation (JST)
Japan

Summary

Redox status changes exert critical impacts on necrotic/apoptotic and normal cellular processes. We report here a widely expressed Ca^{2+}-permeable cation channel, LTRPC2, activated by micromolar levels of H_2O_2 and agents that produce reactive oxygen/nitrogen species. This sensitivity of LTRPC2 to redox state modifiers was attributable to an agonistic binding of nicotinamide adenine dinucleotide (β-NAD^+) to the MutT motif. Arachidonic acid and Ca^{2+} were important positive regulators for LTRPC2. Heterologous LTRPC2 expression conferred susceptibility to death on HEK cells. Antisense oligonucleotide experiments revealed physiological involvement of "native" LTRPC2 in H_2O_2- and TNFα-induced Ca^{2+} influx and cell death. Thus, LTRPC2 represents an important intrinsic mechanism that mediates Ca^{2+} and Na^+ overload in response to disturbance of redox state in cell death.

Introduction

Changes in redox status induce necrotic/apoptotic processes in reperfusion injury during ischemia, degenerative diseases, and normal cellular functions (Coyle and Puttfarcken, 1993; Giroux and Scatton, 1996; Kietzmann et al., 2000). Regulation of intracellular Ca^{2+} concentration ($[Ca^{2+}]_i$) is also critical in both normal and pathological cellular processes (Choi, 1995; Mattson, 1996; Berridge et al., 1998). In acute insults such as hypoxia-ischemia, it has been proposed that the resultant cell fate (necrosis, apoptosis, or survival) is dependent on an intracellular "Ca^{2+} setpoint" (Choi, 1995). Accumulating evidence indicates that cell injury, induced by modification of the redox state, is at least in part due to $[Ca^{2+}]_i$ dyshomeostasis via production of bioactive molecules such as reactive oxygen species (ROS) and reactive nitrogen species (RNS) and their interaction with ion transport mechanisms (Kourie, 1998) including Ca^{2+} channels (Koliwad et al., 1996; Bielefeldt et al., 1997; Klonowski-Stumpe et al., 1997; Kourie, 1998; Lipton and Nicotera, 1998; Li et al., 1998; Mendez and Penner, 1998; Herson et al., 1999). However, the molecular entity of the Ca^{2+} channels activated specifically by disruption of redox state is totally unknown. Furthermore, in nearly all cases, to demonstrate this type of Ca^{2+}-permeable cation current, oxidants such as H_2O_2 at high concentrations (10 mM to 1 M) that would affect at the same time other Ca^{2+} transport mechanisms and ion channels (Kourie, 1998) have been employed (Li et al., 1998; Mendez and Penner, 1998; Herson et al., 1999), while some recent reports have implied that ROS causes $[Ca^{2+}]_i$ elevations at lower concentrations that do not irreversibly damage the cells enough to lead to immediate death (Bielefeldt et al., 1997). Here, we report a novel redox status-dependent Ca^{2+}-permeable cation channel, LTRPC2 (Harteneck et al., 2000), whose intrinsic sensitivity to an activation trigger, β-nicotinamide adenine dinucleotide (β-NAD^+), may underlie susceptibility of cells to death.

Results

LTRPC2 Mediates Ca^{2+} Entry Activated by Micromolar H_2O_2

A phylogenetic tree reveals a gene superfamily for Ca^{2+}-permeable cation channels (Figure 1A). LTRPC2 showed 26% amino acid sequence identity with melastatin (hMLSN-1), while LTRPC2 is distantly related with the classical transient receptor potential (TRP) protein family comprising TRP1–7 (13% identity) and the vanilloid receptors and osmo- and mechano-receptor channels (7%–8% identity) (Harteneck et al., 2000; Inoue et al., 2001), despite its original naming, "TRPC7" (AB001535). Expression of LTRPC2 RNA is widely distributed, being abundant in the lung, spleen, eye, and brain (Figure 1B).

Transient transfection of the human (hLTRPC2) and mouse (mLTRPC2) LTRPC2 cDNA elicited protein expression localized near the plasma membrane in HEK cells together with the transfection marker surface antigen CD8 (Figure 1C). Effects of H_2O_2 on $[Ca^{2+}]_i$ were examined in LTRPC2-expressing cells using fura-2. Surprisingly, 30 μM H_2O_2, which was reported to be insufficient for the immediate death of cells (Bielefeldt et al., 1997), caused a prominent $[Ca^{2+}]_i$ increase within 20 min in 8 out of 66 CD8-positive, LTRPC2-expressing cells. Elevation of the H_2O_2 concentration dramatically short-

[10] Correspondence: moriy@nips.ac.jp

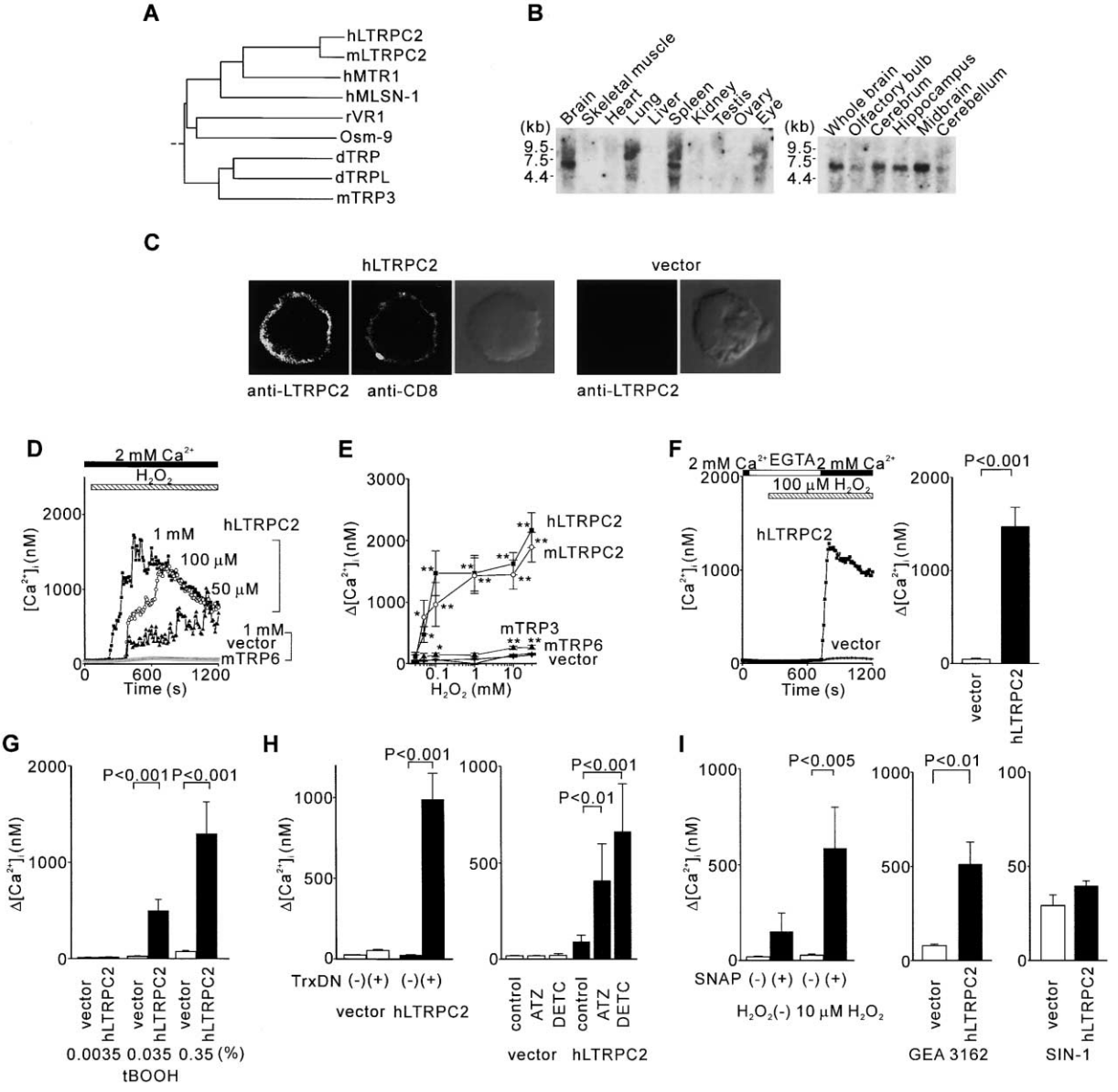

Figure 1. Activation of LTRPC2-Mediated Ca^{2+} Entry by H_2O_2

(A) Phylogenetic tree for the TRP superfamily: hLTRPC2 (GenBank accession No. AB001535), mLTRPC2, human melastatin 1 and TRPC7-related protein 1 (hMTR1) (AF177473), human melastatin 1 (hMLSN-1) (AF071787), rat VR1 (AF029310), *Drosophila* Osm-9 (AF031408), *Drosophila* TRP (M21306), *Drosophila* TRPL (M88185), and mouse TRP3 (mTRP3) (AF190645). The CLUSTAL W program was used.

(B) Northern blot analysis of LTRPC2 RNA distribution in mouse tissues and in the brain.

(C) Confocal immunoimages of LTRPC2 protein localization using an antiserum to the C terminus of mLTRPC2 and FITC-labeled anti-rabbit goat antiserum in hLTRPC2- and vector-transfected HEK cells. Cotransfected CD8 was detected using the monoclonal antibody against human CD8 (B9.2; Immunotech, Marseille, France) and rhodamine-labeled anti-mouse $F(ab')_2$ fragment. The corresponding DIC images are also shown.

(D and E) H_2O_2-induced $[Ca^{2+}]_i$ changes detected in single hLTRPC2-, mLTRPC2-, mTRP3-, mouse TRP6 (mTRP6)-, and vector-transfected HEK cells in the presence of 2 mM extracellular Ca^{2+}. Mean responses (D) and dose-response relationships for maximum $[Ca^{2+}]_i$ rises ($\Delta[Ca^{2+}]_i$) induced by H_2O_2 (E). Data points are the means ± SE $\Delta[Ca^{2+}]_i$. *$p < 0.05$ and **$p < 0.001$, compared with vector-transfected cells.

(F) LTRPC2 mediates Ca^{2+} entry in response to H_2O_2. (left) After 8 min exposure to 100 μM H_2O_2 in Ca^{2+}-free, 0.5 mM EGTA-containing solution, LTRPC2-expressing cells were exposed to the solution containing 2 mM Ca^{2+} and 100 μM H_2O_2. (right) Maximum H_2O_2-induced $[Ca^{2+}]_i$ elevations after readdition of external Ca^{2+}.

(G) $[Ca^{2+}]_i$ elevations induced by tBOOH in LTRPC2-expressing cells in the presence of 2 mM Ca^{2+}.

(H) Perturbation of endogenous antioxidants elicits LTRPC2-mediated $[Ca^{2+}]_i$ elevation in response to H_2O_2 of subthreshold concentration (10 μM). The dominant-negative mutant of thioredoxin was coexpressed (TrxDN) (+), or ATZ (1 mM) and DETC (1 mM) were loaded using nonionic, sulfactant polyol Pluronic F-127 (Molecular Probes, Eugene, OR) 2.5 hr prior to measurements.

(I) Maximum $[Ca^{2+}]_i$ elevations in LTRPC2-expressing cells treated with SNAP (300 μM; left), GEA 3162 (100 μM; middle), or SIN-1 (1 mM; right).

ened latency, prolonged responses, and increased the number of H_2O_2-responsive cells (Figure 1D); 10 mM H_2O_2 induced $[Ca^{2+}]_i$ rises in 92% of LTRPC2-expressing cells. Maximum $[Ca^{2+}]_i$ elevations evoked in LTRPC2-expressing cells showed highly nonlinear dependence on the H_2O_2 concentration (Figure 1E). By contrast, a fewer number of TRP3- or TRP6-expressing cells displayed only small H_2O_2-induced $[Ca^{2+}]_i$ elevations, nearly indistinguishable from those in vector-transfected control cells (Figures 1D and 1E). This excluded the possibility that the observed H_2O_2-induced $[Ca^{2+}]_i$ elevations in LTRPC2-expressing cells were due to nonspecific breakdown of cell membrane and consequent Ca^{2+} influx. It must be noted that TRP3, TRP6, and endogenous capacitative Ca^{2+} entry channels in HEK cells are capable of inducing $[Ca^{2+}]_i$ elevations that reach nearly 600 nM in response to receptor stimulation or store depletion (see Supplemental Figure S1 at http://www.molecule.org/cgi/content/full/9/1/163/DC1; Inoue et al., 2001).

The H_2O_2-induced $[Ca^{2+}]_i$ elevation was observed in LTRPC2-expressing cells only after the addition of Ca^{2+} to external solution (Figure 1F) and was suppressed to 43% ± 10% of control by 100 μM Ni^{2+}. H_2O_2-induced Mn^{2+} influx was markedly enhanced by LTRPC2 expression (Figures 2E and 2F). These results demonstrate that LTRPC2 mediates Ca^{2+} influx in response to H_2O_2 at micromolar levels.

We examined the effects of other oxidants on LTRPC2. *tert*-butyl hydroperoxide (tBOOH) (≥0.035% = 4 mM), which only slightly increased $[Ca^{2+}]_i$ in control cells, induced LTRPC2-mediated $[Ca^{2+}]_i$ elevation with a similar time course as H_2O_2 (Figure 1G). Application of 1 mM dithionite ($Na_2S_2O_4$), which generates superoxide anion (Archer et al., 1995), induced significantly higher $[Ca^{2+}]_i$ elevations (1060 ± 608 nM) in LTRPC2-expressing cells compared to those in control cells (44 ± 6 nM). We also examined whether LTRPC2 channels are activated by perturbation of endogenous levels of ROS (Figure 1H). Coexpression of the dominant-negative mutant of thioredoxin (Ueno et al., 1999), known as a major intracellular antioxidant mechanism together with glutathione, induced LTRPC2-mediated $[Ca^{2+}]_i$ elevation in response to 10 μM H_2O_2, which by itself failed to evoke $[Ca^{2+}]_i$ elevation. Pretreatment with the catalase inhibitor 3-amino-1,2,4-triazole (ATZ; 1 mM) or superoxide dismutase (SOD) inhibitor diethyldithiocarbamic acid (DETC; 1 mM) also elicited $[Ca^{2+}]_i$ elevations via LTRPC2 in response to 10 μM H_2O_2. Previous publications have demonstrated both toxic (Buisson et al., 1992) and protective effects (Wink et al., 1993) of nitric oxide (NO) in ischemia/reperfusion. NO donor *S*-nitroso-*N*-acetyl-DL-penicillamine (SNAP; 300 μM) by itself induced a small LTRPC2-mediated $[Ca^{2+}]_i$ elevation and enhanced its H_2O_2 sensitivity to elicit a $[Ca^{2+}]_i$ response to 10 μM H_2O_2 (Figure 1I). 1,2,3,4-oxatriazolium-5-amino-3-(3,4-dichlorophenyl)-chloride (GEA 3162; 100 μM) potently elevated $[Ca^{2+}]_i$ in LTRPC2-expressing cells, whereas the peroxynitrite donor 3-(4-morpholinyl) sydnonimine hydrochloride (SIN-1; 100 μM, 300 μM, and 1 mM) (Figure 1I) or NO donor 1-hydroxy-2-oxo-3-(3-aminopropyl)-3-isopropyl-1-triazene (NOC 5; 1 mM) was ineffective in inducing or in potentiating $[Ca^{2+}]_i$ elevation (data not shown). Thus, ROS and RNS can activate LTRPC2, although some variability was observed in potency among RNS-generating agents.

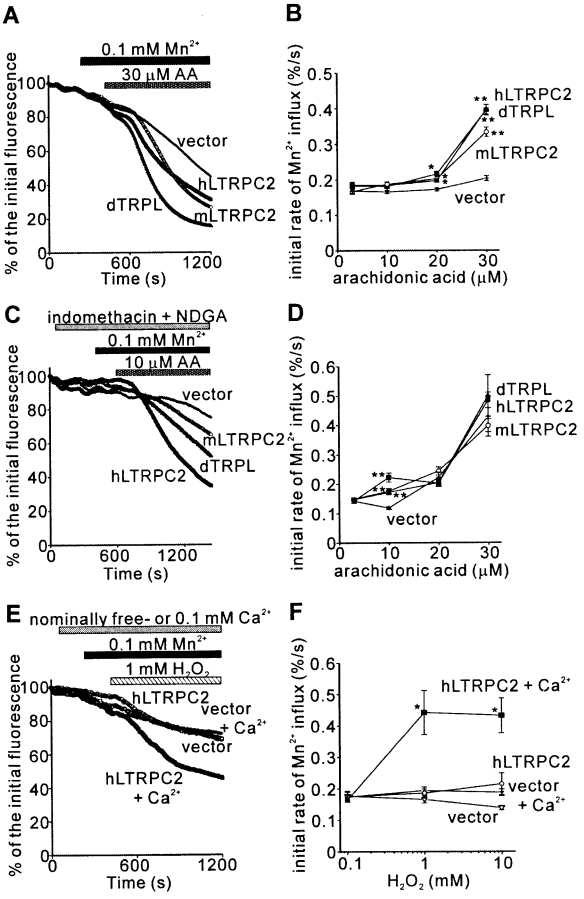

Figure 2. Modulatory Factors of LTRPC2 Activation

(A–D) AA-induced Mn^{2+} influx in hLTRPC2-, mLTRPC2-, *Drosophila* TRPL-, or vector-transfected cells. (A) Quenching of fura-2 fluorescence by Mn^{2+} entry. 30 μM AA was applied after addition of 0.1 mM Mn^{2+} to nominally Ca^{2+}-free HBS. (B) Rates for the initial phase of AA-induced reduction of fluorescence. Data points are the means ± SE percentage reduction of fluorescence (*$p < 0.05$ and **$p < 0.001$). (C) AA-induced Mn^{2+} quenching in the presence of NDGA (20 μM) and indomethacin (20 μM) applied 10 min before AA application (10 μM). (D) Rates for initial phase of AA-induced Mn^{2+} quenching in the presence of the blockers.

(E and F) Dependency of LTRPC2-mediated Mn^{2+} influx on extracellular Ca^{2+}. (E) H_2O_2-induced (1 mM) Mn^{2+} influx was observed in the presence and absence of 0.1 mM Ca^{2+} in hLTRPC2- and vector-transfected cells. (F) Rates for initial phase of H_2O_2-induced Mn^{2+} quenching.

Regulatory Mechanisms of LTRPC2 Activation

Amino acid oxidation modulates various types of Ca^{2+} and K^+ channels (Ruppersberg et al., 1991; Chiamvimonvat et al., 1995; DiChiara and Reinhart, 1997; Li et al., 1998; Xu et al., 1998). However, coexpression of peptide methionine (Met) sulfoxide reductase (MsrA), known to accelerate the inactivation kinetics of A-type K^+ channels (Kuschel et al., 1999), did not suppress the LTRPC2-mediated Ca^{2+} increase induced by 1 mM H_2O_2 (100% ± 7%). The cysteine-specific oxidizing agent 2,2′-dithiobis (5-nitropyridine) (DTBNP; 50 μM) (Li et al.,

1998) elicited similar $[Ca^{2+}]_i$ rises in control (144% ± 3 nM) and LTRPC2-expressing cells (139 ± 4 nM), suggesting that the $[Ca^{2+}]_i$ elevation induced by cysteine oxidation is an endogenous property of HEK cells. Supportively, the typical reducing agent DTT (1 mM), which can reverse amino acid oxidation, failed to suppress the H_2O_2-induced Ca^{2+} influx via LTRPC2 (98% ± 3%). These results suggest that activation of LTRPC2 occurs via characteristic mechanisms distinct from amino acid oxidation.

Our experiments also revealed important modulatory factors for LTRPC2 channels. Arachidonic acid (AA; 30 μM) greatly potentiated Mn^{2+} influx in LTRPC2-expressing cells without H_2O_2, whereas it slightly affected Mn^{2+} influx in control cells (Figures 2A and 2B). The responsiveness of LTRPC2 to AA was comparable to that of TRPL channels (Chyb et al., 1999). The AA-induced Mn^{2+} influx in LTRPC2-expressing cells was not inhibited by the lipoxygenase blocker nordihydroguaiaretic acid (NDGA) or the cyclooxygenase blocker indomethacin (Figures 2C and 2D), suggesting that AA per se, but not its metabolites, is a positive regulator of LTRPC2. H_2O_2-induced Mn^{2+} influx via LTRPC2 was markedly enhanced by extracelluar Ca^{2+} (0.1 mM), which failed to affect Mn^{2+} influx in control cells (Figures 2E and 2F). This is indicative of a positive regulatory role of external Ca^{2+} in LTRPC2 activation by H_2O_2 and contrasts to AA-induced LTRPC2 activation (Figure 2A). In AA stimulation, Ca^{2+} released from internal stores by AA in HEK cells (data not shown) may suffice for LTRPC2 activation in the absence of external Ca^{2+}. Importantly, LTRPC2 did not potentiate $[Ca^{2+}]_i$ elevations induced by stimulation of endogenous G protein-coupled muscarinic receptors (98% ± 8%) (see Supplemental Figures S1A and S1C at http://www.molecule.org/cgi/content/full/9/1/163/DC1) and ATP receptors (98% ± 7%), or by store depletion using thapsigargin (TG) (97% ± 7%) (see Supplemental Figures S1B and S1C at http://www.molecule.org/cgi/content/full/9/1/163/DC1) and cyclopiazonic acid (102% ± 10%), in contrast to TRP3, 5, 6, and 7 in HEK cells (see Supplemental Figure S1A at http://www.molecule.org/cgi/content/full/9/1/163/DC1; Inoue et al., 2001). Thus, LTRPC2 is a novel type of Ca^{2+}-permeable cation channel distinct in activation mechanism from receptor-mediated or store-operated channels.

Agonistic Action of β-NAD^+ Induces Activation of LTRPC2 Channel Currents

To establish channel properties of LTRPC2, ionic currents were examined at a holding potential (V_h) of −50 mV in the nystatin-perforated patch recording (Figure 3A). In 26 out of 54 hLTRPC2-expressing cells, 100 μM H_2O_2 elicited inward currents composed of three phases: the initial lag phase, the slowly developing second phase, and the third phase, which rapidly reached the peak (117 ± 33 pA/pF). Time to reach the peak was 300 ± 23 s, which may imply a gradual accumulation of a direct trigger of the LTRPC2 channel. In TRP3- and TRP6-expressing cells, 100 μM H_2O_2 elicited small inward currents (3 ± 1 and 5 ± 1 pA/pF, respectively; n = 4), but it elicited no detectable currents in control cells (n = 17). The inward current was abolished by replacement of Na^+ with NMDG or by omission of external Ca^{2+} (Figures 3A and 3B), but was unaltered by reduction of the Cl^- concentration (data not shown). The results indicate that Na^+ is the main charge carrier of the LTRPC2 current and were consistent with the importance of extracellular Ca^{2+} as a positive regulator for LTRPC2.

In contrast to the nystatin patch recordings, 100 μM H_2O_2 failed to evoke significant inward currents in the conventional whole-cell configuration (n = 55). This, together with the apparent lack of involvement of Met or Cys oxidation in LTRPC2 activation, implied that a cytoplasmic factor mediates H_2O_2-evoked LTRPC2 activation. Recent publications have demonstrated important roles for NAD^+ as a signaling molecule in physiological functions such as life span extension and monitoring of cellular energy and redox states (Lin et al., 2000; Ziegler, 2000). We presumed NAD^+ was a cytoplasmic activator for LTRPC2, since the oxidized form of NAD^+ could be generated by shift of the redox state to oxidizing by H_2O_2. In fact, using reverse-phase high-performance liquid chromatography (HPLC), we observed an increase of NAD^+ content (from 1.43 ± 0.07 to 2.52 ± 0.18 nmol/mg protein; n = 4) (see Supplemental Figure S2A at http://www.molecule.org/cgi/content/full/9/1/163/DC1) and a decrease of NADH content (from 0.38 ± 0.02 to 0.14 ± 0.01 nmol/mg protein; n = 4) after 5 min exposure to 30 μM H_2O_2 in HEK cells (see Supplemental Figure S2B at http://www.molecule.org/cgi/content/full/9/1/163/DC1). Furthermore, we observed a 25% decrease of NAD(P)H autofluorescence, indicative of an increased $NAD(P)^+$/NAD(P)H ratio in HEK cells incubated with 100 μM H_2O_2 (400 s), as reported previously (Herson et al., 1999; Tretter and Adam-Vizi, 2000). Compared to the oxidants H_2O_2 and tBOOH (0.35%) and RNS-generating agents SNAP and GEA 3162, which effectively activated LTRPC2 (Figure 1I), SIN-1 and NOC 5, which failed to activate LTRPC2 (Figure 1I), elicited a significantly smaller autofluorescence decrease (see Supplemental Figure S3 at http://www.molecule.org/cgi/content/full/9/1/163/DC1). Thus, increase of the $NAD(P)^+$/NAD(P)H ratio correlates well with the potency of the ROS- and RNS-generating agents in evoking LTRPC2 activation.

When hLTRPC2-expressing cells were dialyzed with a patch pipette solution containing 1 mM β-NAD^+, inward currents gradually developed and reached a peak in 9–13 min in 24 out of 124 cells (321 ± 117 pA/pF; maximal response, 1241 pA/pF) (Figure 3C), whereas only 2 out of 14 control cells showed tiny inward currents (2 and 18 pA/pF). A dose-response curve relating β-NAD^+ concentration to the current density demonstrated that LTRPC2 was not activated by β-NAD^+ concentrations of ≤500 μM, but that nearly maximal current amplitude was attained by 3 mM β-NAD^+ and 100% response by 5 mM β-NAD^+ (Figure 3E). The β-NAD^+-induced LTRPC2 currents were also markedly reduced by omission of extracellular Ca^{2+} or by replacement of Na^+ with NMDG (Figure 3C), which excludes the possibility that nonspecific leak currents were evoked by β-NAD^+. The I-V curve of β-NAD^+-induced LTRPC2 currents was linear with a reversal potential of +2.7 ± 0.8 mV (n = 14) (Figure 3D), similar to that of H_2O_2-induced LTRPC2 currents with a reversal potential of −2.7 ± 1.4 mV (n = 6) (Figure 3B). Other β-NAD^+-related molecules, such as NADH (1 mM),

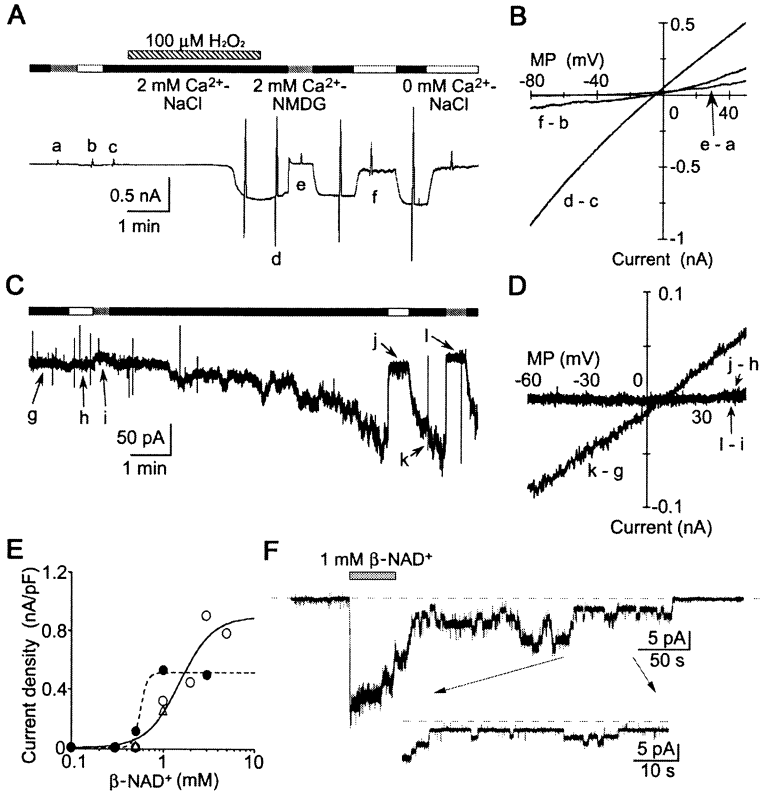

Figure 3. Electrophysiological Characterization of the LTRPC2 Channel

(A–D) Whole-cell LTRPC2 currents induced by H_2O_2 (A) and β-NAD^+ (C). (A) Typical whole-cell currents in nystatin-perforated configuration at a V_h of −50 mV. Two second triangular voltage ramps from −100 to 60 mV were applied. Horizontal bars above each trace indicate the duration of application of the 2 mM Ca^{2+}-NaCl solution (closed bars), 0 mM Ca^{2+}-NaCl solution (open bars), 2 mM Ca^{2+}-NMDG solution (shaded bars), and 100 μM H_2O_2 (hatched bar). (B) I-V relationships of the H_2O_2-induced LTRPC2 current, obtained by subtracting currents before activation of channels from those after activation (indicated by small letters in [A] and [C]). (C) Activation of the LTRPC2 current recorded using the conventional whole-cell mode of patch clamp. 1 mM β-NAD^+ was added to the pipette solution. The current observed within 20 s after the formation of whole-cell configuration was omitted. 0.2 s triangular voltage ramps were applied from a V_h of −50 mV. (D) I-V relationships of the β-NAD^+-induced LTRPC2 current.

(E) Dose-response curve relating intrapipette β-NAD^+ concentration to LTRPC2 current density (open circles) (apparent K_D, 1.8 mM; Hill coefficient, 2.2) and that obtained when AA was applied (closed circles) (apparent K_D, 0.56 mM; Hill coefficient, 11.5). Open triangles are current densities obtained by dialyzing cells with β-NAD^+ plus NADH (50 μM), $NADP^+$ (70 μM), NADPH (50 μM), ADP (800 μM), and ATP (2 mM) from the patch pipette.

(F) Activation of single LTRPC2 channel currents by β-NAD^+ in cell-free, excised inside-out membrane patches at a V_h of −50 mV. The segment indicated by the arrows is expanded on a faster time scale (inset).

$NADP^+$ (3 mM), and cADP ribose (20 μM), failed to activate the LTRPC2 channel. In addition, other physiological cellular components, NADH (50 μM), $NADP^+$ (70 μM), NADPH (50 μM), ADP (800 μM), and ATP (2 mM) (Dunne et al., 1988), in the pipette did not affect the LTRPC2 activity evoked by 1 mM β-NAD^+, while they slightly lowered the threshold for LTRPC2 activation to elicit small LTRPC2 currents in response to 500 μM β-NAD^+ (7.7 ± 1.1 pA/pF; n = 4) (Figure 3E). Three millimolar β-NAD^+ with 10 mM BAPTA in the pipette solution evoked no significant inward LTRPC2 currents. Since $[Ca^{2+}]_i$ elevation by TG or receptor stimulation failed to activate LTRPC2 (see Supplemental Figure S1 at http://www.molecule.org/cgi/content/full/9/1/163/DC1) (data not shown), the result suggests that Ca^{2+} is necessary but not sufficient for LTRPC2 activation. Furthermore, extracellular application of 10 μM AA shifted dependence of LTRPC2 currents on β-NAD^+ toward lower concentrations and suppressed maximal LTRPC2 current amplitudes (Figure 3E), revealing an interesting modulatory effect of AA that enhances β-NAD^+ sensitivity of LTRPC2.

Direct Interaction of β-NAD^+ with MutT Motif Is Critical for LTRPC2 Activation

Structural comparison of LTRPC2 with other proteins revealed an amino acid sequence homologous to the "MutT" module, which is conserved among the active sites of nucleoside diphosphate hydrolyzing enzymes (Bessman et al., 1996) in the putatively cytoplasmic C-terminal region (Figure 4A). The LTRPC2 construct with a deletion of the MutT sequence showed no detectable Ca^{2+} influx activity in response to H_2O_2 up to 30 mM (Figure 4C) and slightly but significantly reduced Mn^{2+} influx activity in response to AA (Figure 4D). Since replacing the Met residue (M1397) with isoleucine in the MutT motif (M1397I) only slightly affected the LTRPC2 activity, oxidation of M1397 is not an absolute requirement for LTRPC2 activation. In the putatively cytoplasmic N terminus, we also found a sequence that resembles the charged region responsible for the stimulation of the two-pore domain TREK-1 K^+ channel by AA (Figure 4B) (Patel et al., 1998). Deletion of the motif (AA-responsive sequence [ARS]) abrogated responsiveness of LTRPC2 to both AA and H_2O_2 (Figures 4C and 4D). The deletion mutants elicited no significant inward currents in cells dialyzed with 3 or 30 mM β-NAD^+ despite localization near the plasma membrane (see Supplemental Figure S4A at http://www.molecule.org/cgi/content/full/9/1/163/DC1; compare wild-type in Figure 1C). Thus, MutT and ARS are critical structural bases for β-NAD^+- and AA-dependent activation of LTRPC2 channels.

Two additional experiments supported direct interaction of β-NAD^+ with the LTRPC2 protein. First, inward currents were immediately induced by β-NAD^+ applied from the cytoplasmic side of inside-out membrane patches excised from hLTRPC2-expressing cells (Figure

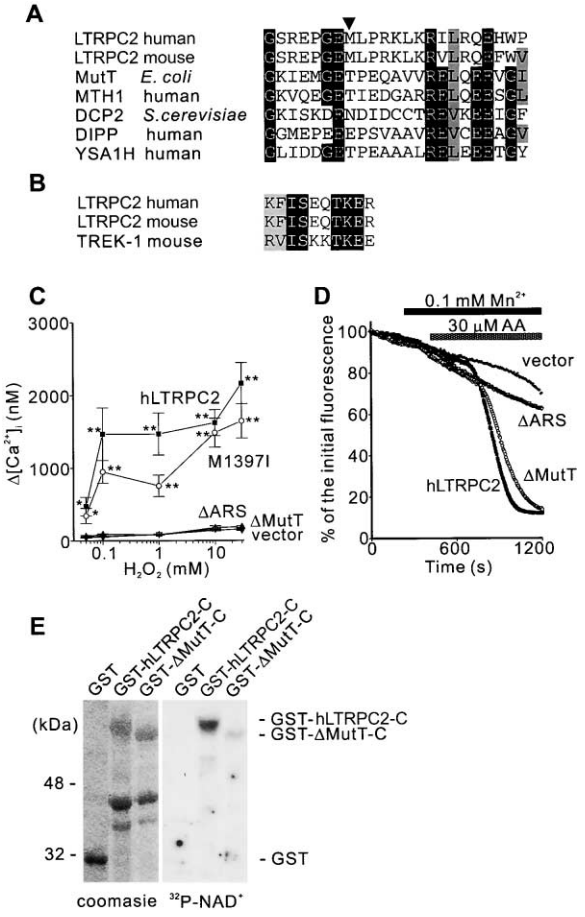

Figure 4. The MutT Motif and AA-Responsive Sequence (ARS) Are Essential for Activation of the LTRPC2 Channel

(A) Alignment of the MutT sequences in hLTRPC2 (residues 1390–1412) and mLTRPC2 (residues 1386–1408) with those in *E.coli* MutT (P08337), human MTH1 (AB025233), *S. cerevisiae* DCP2 (YSCPSU1A), human diphosphoinositol polyphosphate phosphohydrolase (DIPP) (AF062529), and human YSA1H (AF155832). The residues well conserved among the aligned sequences and the bulky aliphatic amino acids are indicated by black and gray boxes, respectively. The arrowhead indicates M1397.

(B) Alignment of the ARS in hLTRPC2 (residues 307–316), mLTRPC2 (residues 306–315), and TREK-1 (residues 297–306) (Patel et al., 1998). The conserved residues and chemically similar residues are indicated by black and gray boxes, respectively.

(C) H_2O_2 concentration dependence of maximum $[Ca^{2+}]_i$ elevations in hLTRPC2-, M1397I-, ΔARS-, ΔMutT-, and vector-transfected cells. The MutT (residues 1390–1409) or ARS (residues 307–316) was deleted in ΔMutT or ΔARS, respectively. Data points are the means ± SE $\Delta[Ca^{2+}]_i$. *$p < 0.05$ and **$p < 0.001$.

(D) AA-induced (30 μM) Mn^{2+} influx in hLTRPC2-, ΔMutT-, ΔARS-, and vector-transfected cells.

(E) β-NAD^+ binding assay. Total proteins from *E. coli* expressing the GST protein (GST) and the GST fusion proteins for the intact (GST-hLTRPC2-C) and MutT-deleted hLTRPC2 C terminus (GST-ΔMutT-C) were fractionated by 12.5% SDS-polyacrylamide gel (equal amount of GST proteins was applied) and stained with Coomassie brilliant blue (left) or transferred to nitrocellulose membrane for a subsequent binding experiment (right). The membrane was incubated with [^{32}P]NAD^+, washed, and subjected to autoradiography.

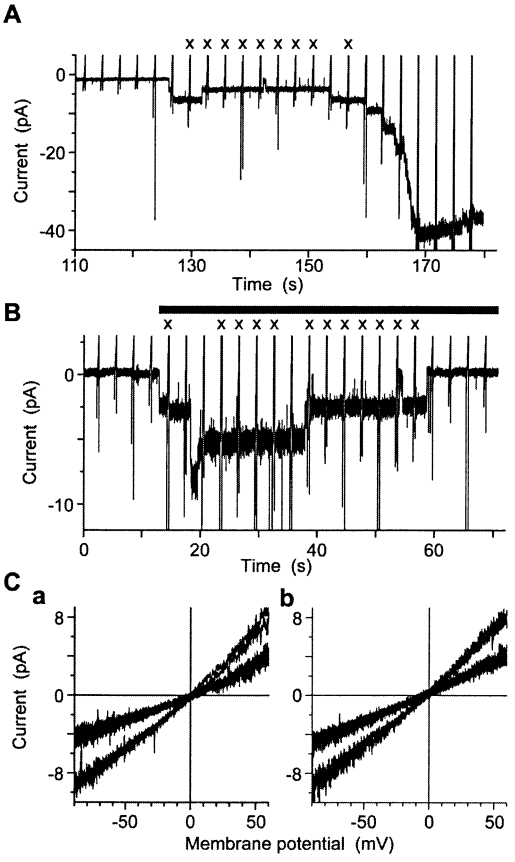

Figure 5. Single-Channel Properties of the LTRPC2 Channel

(A) Single-channel currents recorded at a V_h of −50 mV in cell-attached patch configuration from hLTRPC2-expressing cells continuously treated with 100 μM H_2O_2 from outside the patch. The trace without unitary activity for the initial 110 s H_2O_2 application was omitted. 330 ms triangular voltage ramps from −90 mV to 60 mV were applied every 3 s.

(B) Single-channel currents activated at a V_h of −50 mV by 3 mM β-NAD^+ applied to the inner surface of the patch membrane excised from LTRPC2-expressing cells in inside-out patch configuration. The same voltage ramps as in (A) were applied.

(C) Subtracted I-V relationships of the single LTRPC2 channel. (a) and (b) are from (A) and (B), respectively. The average of currents at the level 0 was subtracted from the currents with marks (x) at the level 1 or 2.

3F). After omission of β-NAD^+, the activity sustained itself but gradually diminished, and unitary opening events became resolvable (Figure 3F). By contrast, no similar unitary activity was observed in the excised patches from control cells (n = 20). Unitary LTRPC2 currents were also recorded from a cell-attached patch in H_2O_2-treated LTRPC2-expressing cells (Figure 5A). When the patch was pulled off and excised as a inside-out patch, the activity disappeared, but it was restored by application of 3 mM β-NAD^+ instead of H_2O_2 (Figure 5B). The H_2O_2-induced and β-NAD^+-activated unitary activities showed similar long openings and linear I-V relationships, reminiscent of those of whole-cell currents (Figure 3B and 3D). Unitary conductance of the H_2O_2-induced channel (52.3 ± 2.8 pS) and that of the β-NAD^+-activated channel (59.0 ± 1.3 pS) showed no statistically significant difference. Omission of Ca^{2+} from

the solution perfused on inside-patches using 10 mM BAPTA abolished the β-NAD^+-induced activity, leading to the idea that extracellular Ca^{2+} required for activation passes through the LTRPC2 channel to act from the intracellular side. The results strongly suggest an identity of the β-NAD^+-activated channel with the H_2O_2-activated channel in LTRPC2-expressing cells. Second, biochemical experiments demonstrated direct interaction of β-NAD^+ with LTRPC2 (Figure 4E). ^{32}P-labeled β-NAD^+ showed potent binding to the GST fusion protein of the hLTRPC2 C terminus, but much weaker binding to the fusion protein with the MutT deletion, suggesting a secondary interaction between chemical groups other than nucleotide diphosphate of β-NAD^+ with a LTRPC2 structure outside MutT. The results together support that direct action of β-NAD^+ to the MutT motif mediates activation of the Ca^{2+}- and Na^+-permeable cation channel LTRPC2.

Heterologous LTRPC2 Expression Confers Susceptibility to H_2O_2-Induced Cell Death

LTRPC2-expressing cells were significantly susceptible to cell death induced by exposure to H_2O_2 (≥10 μM) in trypan blue exclusion assays (Figure 6A) and to reduction of cell survival by H_2O_2 (≥50 μM) in mitochondrial dehydrogenase activity assays (Figure 6C). In 4 out of 44 hLTRPC2-expressing cells, which showed $[Ca^{2+}]_i$ elevation, cell death assessed by propidium iodide (PI) staining was simultaneously observed after 30 min exposure to 100 μM H_2O_2 (Figure 6D), but $[Ca^{2+}]_i$ response or death was undetectable in control cells. By contrast, with LTRPC2 in Ca^{2+}-free external solution (or the MutT- and ARS-deleted mutants), TRP3 or TRP6 conferred on HEK cells only marginal susceptibility, if at all, to the impairment of trypan blue exclusion by H_2O_2 (≥1 mM) (Figures 6A and 6B). Transfection of TRP3, TRP6, and vector elicited a smaller reduction in viability induced by H_2O_2 (≥300 μM) (Figure 6C). In support of a direct correlation between $[Ca^{2+}]_i$ elevation and cell death, H_2O_2 applied with 10 μM BAPTA-AM failed to induce cell death (Figure 6B). Cytoplasmic budding was already observed in 68% of LTRPC2-expressing cells treated with 100 μM H_2O_2 (Figures 6E and 6F), whereas the majority of TRP3- and TRP6-expressing cells and control cells were free from the prominent morphological change, except for 72% of the TRP3-expressing cells treated with 10 mM H_2O_2 (Figure 6F). It must be noted that 20 min stimulation of TRP3- and TRP6-expressing cells with 30 μM carbachol did not impair trypan blue exclusion, and TRP3, TRP6, and LTRPC2 showed similar expression levels (3.8, 4.1, and 2.9 pmol/1 × 10^5cells for mTRP3, mTRP6, and hLTRPC2, respectively) and plasma membrane localization (see Supplementary Figure S4D at http://www.molecule.org/cgi/content/full/9/1/163/DC1). Furthermore, activation of caspase-3 and DNA laddering were not induced in hLTRPC2-expressing cells by 100 or 300 μM H_2O_2. Thus, heterologous LTRPC2 channels are capable of mediating H_2O_2-induced cell death.

Ca^{2+} Influx and Cell Death Mediated by LTRPC2 in Native Systems

To investigate physiological functions of LTRPC2 channels in "native" systems, LTRPC2 expression was suppressed by treatment with an antisense oligonucleotide. In rat insulinoma RIN-5F cells (Herson et al., 1999), the antisense oligonucleotide, which dramatically diminished LTRPC2 immunoreactivity localized near the plasma membrane and in the cytoplasmic area (Figure 7A), significantly suppressed Ca^{2+} influx (Figure 7C) and cell death (Figure 7D) induced by H_2O_2, in clear contrast with the sense oligonucleotide. TNFα evoked $[Ca^{2+}]_i$ oscillation in RIN-5F cells (Figure 7E). LTRPC2 antisense almost abolished this $[Ca^{2+}]_i$ response, as observed for omission of extracellular Ca^{2+} (Figure 7E). Strikingly, the antisense treatment significantly suppressed TNFα-induced death in RIN-5F cells (Figure 7F). Suppression of TNFα-induced death was achieved also in the presence of intracellular Ca^{2+} chelator BAPTA-AM and antioxidant glutathione, consistent with the critical role of Ca^{2+} and ROS in LTRPC2-mediated death. TNFα- and H_2O_2-induced cell death was similarly suppressed by the antisense treatment in the monocyte cell line U937 (Figure 7G). The results suggest important involvement of LTRPC2 in formation of native H_2O_2-activated Ca^{2+} channels that mediate cell death.

Discussion

The present investigation reveals that LTRPC2 is the molecular entity of Ca^{2+}- and Na^+-permeable cation channels activated via agonistic binding of β-NAD^+ in response to changes in redox status. Our measurement of cellular NAD^+ levels and the previous estimation of the basal NAD^+ concentration as ranging from 200 to 350 μM (Dunne et al., 1988) suggest that NAD^+ concentration elevated by H_2O_2 to the threshold near 500 μM mediates LTRPC2 activation. In fact, the potency of oxidants and RNS-generating agents in activating LTRPC2 channels shows good correlation with their ability to increase $NAD(P)^+$/NAD(P)H. However, it is also possible that as an allosteric effector, NAD^+ enhances the agonistic action of other factors such as AA. Since the effect of H_2O_2 on LTRPC2 was observed only in the electrophysiological technique that retains the intracellular structure and composition, it is unlikely that direct action of ROS, protein modification, or membrane peroxidation by itself is sufficient for LTRPC2 activation, although basal oxidation at a redox site in LTRPC2 not reached by extracellularly applied DTT may be involved in the activation. The results also indicate impairment of AA and H_2O_2 sensitivity by deletion of ARS in LTRPC2 channels, suggesting that AA is essential for β-NAD^+-dependent activation of LTRPC2. Endogenous AA may keep the activation threshold of LTRPC2 channels within a range of intracellular β-NAD^+ concentrations that H_2O_2 elevates, and exogenous AA may shift the threshold toward lower β-NAD^+ concentrations to facilitate current activation. Since H_2O_2 treatment has been reported to produce AA (Barlow et al., 2000), the β-NAD^+ concentration-dependence lowered by AA may be involved in H_2O_2-induced LTRPC2 activation. Thus, LTRPC2 should be functionally categorized in a novel group of Ca^{2+} channels, distinct from STRPs and OTRPs (Harteneck et al., 2000). Since submission of this manuscript, two other papers on LTRPC2 appeared (Perraud et al., 2001; Sano et al., 2001). Our data is consistent with the papers

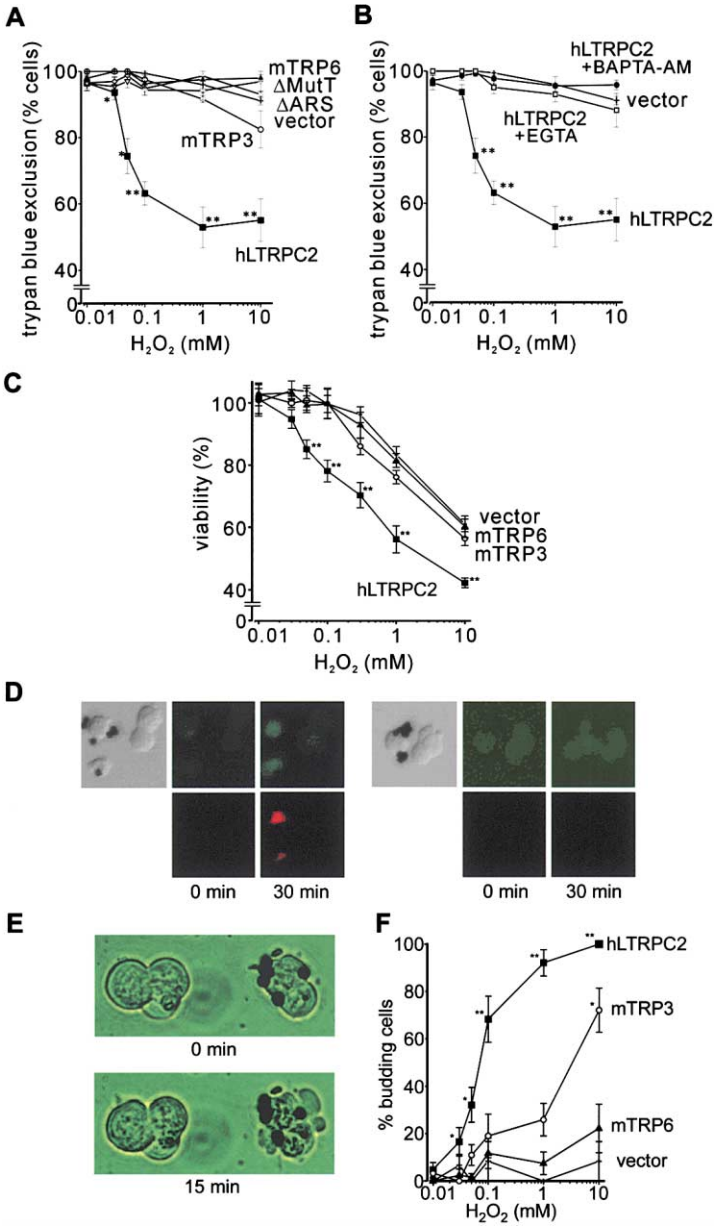

Figure 6. LTRPC2 Confers Susceptibility to H_2O_2-Induced Death

(A and B) Viability assessed by trypan blue exclusion. Cells transfected with hLTRPC2, ΔMutT, ΔARS, mTRP3, mTRP6, and vector were exposed to H_2O_2 in HBS, Ca^{2+}-free HBS, or BAPTA-AM-containing HBS solution for 20 min. Data points are the means ± SE from 4 to 15 experiments.

(C) Viability assessed by the MTT assay. Cells transfected with hLTRPC2, mTRP3, mTRP6, and vector were exposed to H_2O_2 (1 hr). The data were normalized by those measured in untreated cells. Each data point was obtained from 6 to 17 experiments.

(D) Simultaneous detection of H_2O_2-induced $[Ca^{2+}]_i$ changes (upper panels) and cell death (lower panels) by observing confocal fluorescent images of fluo-3 and PI, respectively, in hLTRPC2-transfected cells. (left panels) Both $[Ca^{2+}]_i$ elevation and cell death were induced. (right panels) Only $[Ca^{2+}]_i$ elevation was detected.

(E and F) H_2O_2-induced membrane budding. (E) Cells were incubated with H_2O_2 (100 μM) and Ca^{2+} (2 mM) for 15 min. Membrane budding was observed in LTRPC2-expressing cells attached with anti-CD8 antibody-coated beads (right), but not in CD8-negative cells (left). (F) Percentages of budding cells in hLTRPC2-, mTRP3-, mTRP6-, and vector-transfected cells after 15 min exposure to H_2O_2 (10 μM to 10 mM). *$p < 0.05$ and **$p < 0.001$.

in most functional aspects, including linear I-V curves and activation triggers, except for the lack of inhibition by internal ATP, which may be due to our combining ATP with other physiological components (Figure 3E).

Antisense experiments suggest involvement of LTRPC2 in native H_2O_2-induced Ca^{2+} influx and cell death. Herson et al. (1999) previously reported a β-NAD^+-activated nonselective cation (NS_{NAD}) channel induced by H_2O_2 in CRI-G1 rat insulinoma cells. The immediate and complete cessation of H_2O_2-induced NS_{NAD} channel activity by patch excision, linear I-V relationships, and lack of selectivity among cations are similar to what we observed for LTRPC2, suggesting that the NS_{NAD} channel represents the native LTRPC2 channel. Higher H_2O_2 and Ca^{2+} requirements of NS_{NAD} channels compared with those of LTRPC2 may be attributable to multimerization of LTRPC2 with other subunits or intracellular modulatory components in native systems. Nonselective cation channels activated under UV irradiation and oxidant stress by H_2O_2 and tBOOH of relatively high concentrations or by oxidized glutathione have been reported in various mammalian cells (Koliwad et al., 1996; Mendez and Penner, 1998). Since these cation channels survive in excised inside-out patches, they would be activated via a membrane-delimited pathway (Mendez and Penner, 1998) and may rather represent native counterparts of TRP3 and TRP6.

LTRPC2, which efficiently transforms changes in redox status to Ca^{2+} overload, is of great pathophysiological importance because it enables cell injury to directly affect and shift the intracellular Ca^{2+} setpoint, on which the resultant fate of the cell depends (Choi, 1995; Lipton and Nicotera, 1998). The results also indicate that LTRPC2 conducts a large amount of Na^+, which, in com-

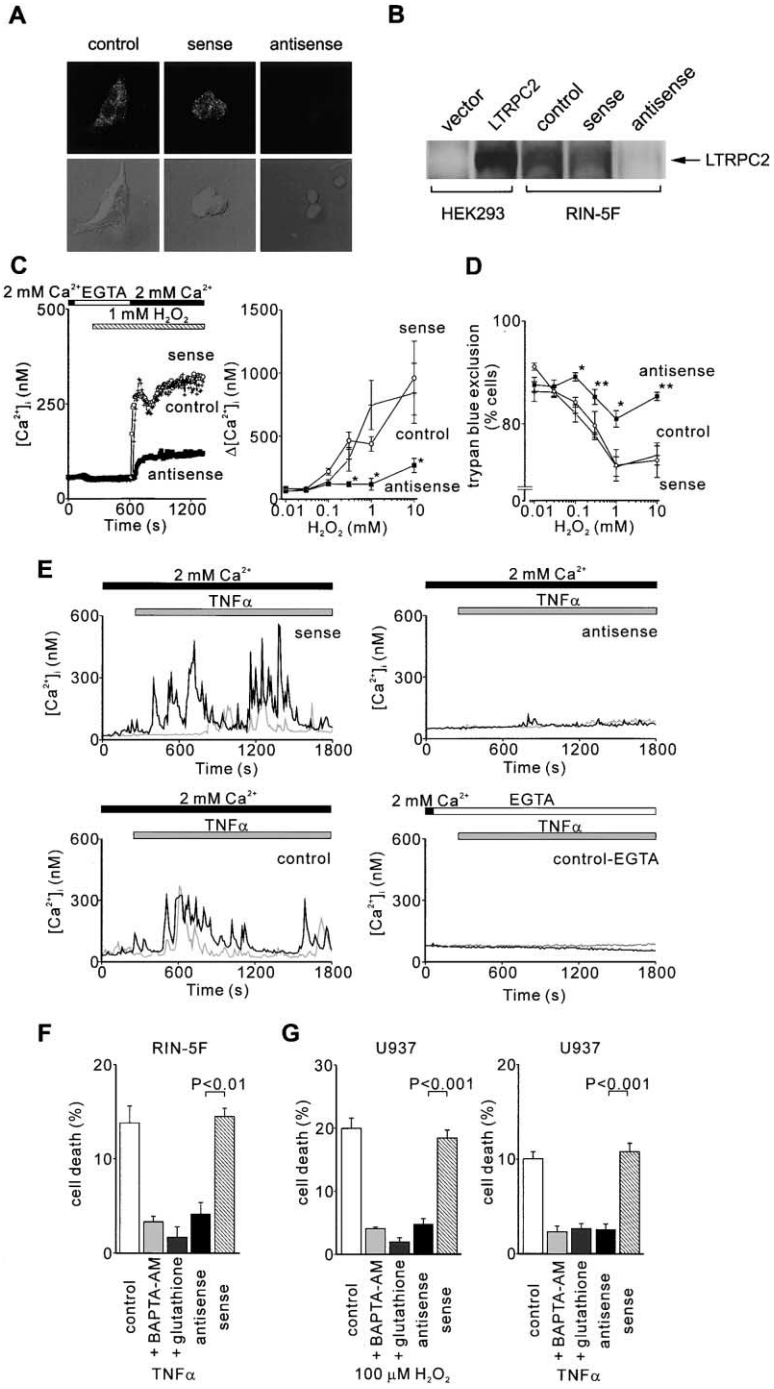

Figure 7. Ca^{2+} Influx and Cell Death Mediated by Native LTRPC2

(A and B) LTRPC2 protein in rat insulinoma RIN-5F cells. (A) Confocal immunoimages of LTRPC2 (upper panels) and the corresponding DIC images of differential interference contrast (lower panels) in control (left) and sense oligonucleotide- (middle) or antisense oligonucleotide-treated RIN-5F cells (right). (B) Western blot analysis of LTRPC2 expression in RIN-5F and hLTRPC2-transfected HEK cells.

(C) (left) Ca^{2+} entry induced in LTRPC2 oligonucleotide-treated and control RIN-5F cells after 6 min exposure to 1 mM H_2O_2 in the absence of external Ca^{2+}. (right) The maximum H_2O_2-induced $[Ca^{2+}]_i$ elevations due to Ca^{2+} entry. *$p < 0.05$ compared with control cells.

(D) Viability assessed by trypan blue exclusion during exposure to H_2O_2 in LTRPC2 sense- or antisense-treated and control RIN-5F cells. *$p < 0.05$ and **$p < 0.001$.

(E and F) Effects of antisense or sense treatment on oscillatory $[Ca^{2+}]_i$ responses (E) and cell death (F) induced by TNFα ([E], 1 μg/ml; [F], 100 ng/ml) in RIN-5F cells. Effects of coincubation with EGTA (E) and with 1 μM BAPTA-AM or 1 mM glutathione are also shown (F).

(G) Effects of antisense or sense treatment and of BAPTA-AM or glutathione on cell death induced by TNFα and H_2O_2 in U937 cells. In (F) and (G), percentages of cells that showed impaired trypan blue exclusion are indicated.

bination with oxidative stress, is important in neuronal injury (Friedman and Haddad, 1993; Mattson, 1996). These features and wide tissue distribution suggest general significance of LTRPC2 in cell death and degenerative diseases. Since far less sensitivity to H_2O_2-induced death was conferred by TRP3 and TRP6 in the presence of extracellular Ca^{2+} or by LTRPC2 in the absence of Ca^{2+} (Figure 6), it is improbable that LTRPC2-mediated cell death is due to nonspecific effects of membrane depolarization by overexpressed Ca^{2+}-permeable cation channels. The LTRPC2-mediated mechanism is different from nonspecific disruption of the cell membrane integrity through lipid peroxidation or even from Ca^{2+}-permeable cation currents induced by UV or oxidizing agents (Mendez and Penner, 1998), as discussed above. The mechanism is also distinct from the hypothesis that ROS causes DNA strand breaks, activation of nuclear poly (ADP-ribose) polymerase, and depletion of β-NAD^+, leading to cell death (Okamoto, 1985). Importantly, cell death in HEK cells mediated by LTRPC2 was not accompanied by DNA fragmentation or activation of caspase-3. This is unlikely to derive from the transient nature of our expression system, since transfection efficiency exceeding 20% should allow detection of DNA laddering.

An alternative possibility that HEK cells are intrinsically insusceptible to apoptosis can be also excluded, since DNA fragmentation was induced in HEK cells by staurosporine (Y.H. and Y.M., unpublished data). Thus, the form of LTRPC2-mediated cell death may be necrotic or caspase independent.

Experimental Procedures

Molecular cloning and recombinant expression of LTRPC2 and details of immunofluorescence staining and fluorescent and electrophysiological measurements can be accessed at http://www.molecule.org/cgi/content/full/DC1.

Molecular Cloning and Recombinant Expression in HEK293 Cells

Recombinant pCI-neo plasmids (Promega, Madison, WI) containing LTRPC2 cDNAs, isolated by PCR amplification and by screening a mouse brain cDNA library, were expressed in HEK cells. Mutants were constructed using PCR techniques.

Immunofluorescence Staining

Anti-mouse LTRPC2 rabbit antiserum (mLTRPC2-C1) was directed against the C terminus 1488–1506 (YANHKTILQKVASLFGAHF). The fluorescence immunoimages were acquired with a confocal laser scanning microscope (LSM 510, Zeiss, Oberkochen, Germany) equipped with a krypton/argon ion laser. The emitted fluorescence was collected through an objective lens with a 63× and 86× magnification for HEK and RIN-5F cells (ATCC, Manassas, VA), respectively.

Fluorescent Measurements and Electrophysiology

The fura-2 fluorescence was measured in HEPES-buffered saline (HBS) containing 107 mM NaCl, 6 mM KCl, 1.2 mM $MgSO_4$, 2 mM $CaCl_2$, 11.5 mM glucose, and 20 mM HEPES (adjusted to pH 7.4 with NaOH). The 340:380 nm ratio images were converted to Ca^{2+} concentrations by in vivo calibration (Nishida et al., 1999) using 5 μM ionomycin. Fluorescence quenching by Mn^{2+} entry was studied using the fura-2 isosbestic excitation wavelength at 360 nm. NAD(P)H autofluorescence of HEK cells was observed using excitation at 360 nm and emission at 460 nm (Eng et al., 1989). Whole-cell currents were recorded using the nystatin-perforated patch technique or the conventional whole-cell configuration, as in Inoue et al. (2001). The pipette solution was 150 mM CsCl, 2 mM $MgCl_2$, 5 mM EGTA, and 5 mM HEPES (adjusted to pH 7.2 with CsOH). The 0 mM Ca^{2+}-NaCl solution contained 121.7 mM NaCl, 1.2 mM $MgCl_2$, 1.2 mM $CaCl_2$, 2 mM EGTA, 10 mM glucose, 11.5 mM HEPES, and 51 mM mannitol (adjusted to pH 7.4 with NaOH; 90 nM calculated free Ca^{2+}). The 2 mM Ca^{2+}-NaCl solution contained 125 mM NaCl, 1.2 mM $MgCl_2$, 2 mM $CaCl_2$, 10 mM glucose, 11.5 mM HEPES, and 51 mM mannitol (adjusted to pH 7.4 with NaOH). The 2 mM Ca^{2+}-NMDG solution was made by the substitution of equimolar NMDG-Cl for NaCl. For the inside-out and cell-attached patch recordings, the recording pipette contained the 2 mM Ca^{2+}-NaCl solution, and the bathing solution contained 155 mM KCl, 0.581 mM $CaCl_2$, 2 mM $MgCl_2$, 2 mM EGTA, and 5 mM HEPES (adjusted to pH 7.25 with KOH; 50 nM calculated free Ca^{2+}).

Analysis of Pyridine Dinucleotide in HEK Cells by HPLC

NAD^+ and NADH contents were measured using reversed-phase HPLC with a modification by Litt et al. (1989). For determination of NAD^+ and NADH, a 500 μl aliquot from the 2 ml cell suspension of a 10 cm dish culture was treated with 50 μl of 3 M perchloric acid and 0.5 M NaOH/50% (v/v) ethanol/35% CsCl, respectively. After a 10 min centrifugation at 15,000 rpm, supernatants were separated on a TSK-Gel ODS-80Ts (4.6 × 250 mm) column (Tosoh, Tokyo, Japan). The mobile phase was 0.1 M KH_2PO_4 (pH 6.0)/5% methanol. NAD^+ and NADH were identified by UV detection (254 nm) and fluorometric detection (Excitation 370 nm, Emission 460 nm), respectively. Protein contents were determined by *Dc* Protein Assay Kit (Bio-Rad, Hercules, CA).

β-NAD^+ Binding Assay

pGEX-4T-3 (Amersham Pharmacia, Buckinghamshire, UK) was used for GST constructs. Total proteins from *E. coli* (BL-21) expressing GST fusion proteins for the hLTRPC2 C terminus (residues 1286–1503) and those with the MutT deletion (residues 1390–1409) (ΔMutT) were fractioned by 12.5% SDS-polyacrylamide gel and blotted to nitrocellulose membrane. Blots were incubated with 5 μl of [^{32}P]β-NAD^+ (29.6 TBq/mmol, 185 MBq/ml) (NEN, Tokyo, Japan) in 10 ml of binding buffer (1 mM EDTA, 5 mM $MgCl_2$, 1% Tween 20, and 50 mM Tris-HCl [pH 7.5]) for 90 min and were washed twice with binding buffer at room temperature. Autoradiography was performed at −70°C for 2 days with an intensifying screen.

Assays for Cell Death

Cell death was induced in HEK cells 36 hr after transfection. Viability was assessed by the colorimetric 3-(4,5-dimethylthiazol-2-yl)-2,5-diphenyl tetrazolium bromide (MTT) assay and by trypan blue exclusion (Maeno et al., 2000). Changes in $[Ca^{2+}]_i$ and cell death were assessed simultaneously by observing emission of fluo-3 and PI under a confocal microscope (Shimizu et al., 1998). To induce death of RIN-5F and U937 cells, 100 ng/ml TNFα with 1 ng/ml cycloheximide or 100 μM H_2O_2 was applied (6 hr) in 0.5% FBS-containing RPMI 1640.

Antisense Oligonucleotide Experiments

Cells were maintained with either antisense or sense oligonucleotides (5 μM) in RPMI 1640 containing 1% FBS plus antibiotics for 5 days. Alternatively, cells were maintained with oligonucleotide (20 nM) and Oligofectamine Reagent (Invitrogen, Carlsbad, CA) for 4 hr in FBS- and antibiotic-free RPMI 1640 to which 10% FBS was supplemented for next 36 hr. Adherent cells were trypsinized and reseeded on cover slips in the medium containing oligonucleotides and used within 6–24 hr for assays. The antisense and sense oligonucleotides used were 5′-ACGATGTCACCAAAGGCATC-3′ and 5′-GAT GCCTTTGGTGACATCGT-3′, respectively, for RIN-5F, and 5′-CTC AGGGCTGAGGGCTCCAT-3′ and 5′-ATGGAGCCCTCAGCCCTGAG-3′, respectively, for U937.

Western Blot Analysis

The lysates of HEK cells harvested 48 hr after transfection were fractionated by 8% SDS-polyacrylamide gel and transferred to nitrocellulose membrane as previously described (Inoue et al., 2001). Blots were incubated with anti-mLTRPC2-C1 antiserum and stained using the ECL Western blotting analysis system (Amersham Pharmacia).

Acknowledgments

We thank H. Bito, M. Yamada, and Y. Kiuchi for helpful advice and K. Saito, N. Sekiguchi, and A. Nishihashi for technical assistance. This work was supported by a research grant from the Ministry of Education, Culture, Sports, Science, and Technology and by the "Research for the Future" program of the Japan Society for the Promotion of Science.

Received May 30, 2001; revised November 13, 2001.

References

Archer, S.L., Hampl, V., Nelson, D.P., Sidney, E., Peterson, D.A., and Weir, E.K. (1995). Dithionite increases radical formation and decreases vasoconstriction in the lung. Evidence that dithionite does not mimic alveolar hypoxia. Circ. Res. *77*, 174–181.

Barlow, R.S., El-Mowafy, A.M., and White, R.E. (2000). H_2O_2 opens BK_{Ca} channels via the PLA_2-arachidonic acid signaling cascade in coronary artery smooth muscle. Am. J. Physiol. *279*, H475–H483.

Berridge, M.J., Bootman, M.D., and Lipp, P. (1998). Calcium—a life and death signal. Nature *395*, 645–648.

Bessman, M.J., Frick, D.N., and O'Handley, S.F. (1996). The MutT proteins or "Nudix" hydrolases, a family of versatile, widely distributed, "housecleaning" enzymes. J. Biol. Chem. *271*, 25059–25062.

Bielefeldt, K., Whiteis, C.A., Sharma, R.V., Abboud, F.M., and Conk-

lin, J.L. (1997). Reactive oxygen species and calcium homeostasis in cultured human intestinal smooth muscle cells. Am. J. Physiol. *272*, G1439–G1450.

Buisson, A., Plotkine, M., and Boulu, R.G. (1992). The neuroprotective effect of a nitric oxide inhibitor in a rat model of focal cerebral ischaemia. Br. J. Pharmacol. *106*, 766–767.

Chiamvimonvat, N., O'Rourke, B., Kamp, T.J., Kallen, R.G., Hofmann, F., Flockerzi, V., and Marban, E. (1995). Functional consequences of sulfhydryl modification in the pore-forming subunits of cardiovascular Ca^{2+} and Na^{+} channels. Circ. Res. *76*, 325–334.

Choi, D.W. (1995). Calcium: still center-stage in hypoxic-ischemic neuronal death. Trends Neurosci. *18*, 58–60.

Chyb, S., Raghu, P., and Hardie, R.C. (1999). Polyunsaturated fatty acids activate the *Drosophila* light-sensitive channels TRP and TRPL. Nature *397*, 255–259.

Coyle, J.T., and Puttfarcken, P. (1993). Oxidative stress, glutamate, and neurodegenerative disorders. Science *262*, 689–695.

DiChiara, T.J., and Reinhart, P.H. (1997). Redox modulation of *hslo* Ca^{2+}-activated K^{+} channels. J. Neurosci. *17*, 4942–4955.

Dunne, M.J., Findlay, I., and Petersen, O.H. (1988). Effects of pyridine nucleotides on the gating of ATP-sensitive potassium channels in insulin secreting cells. J. Membr. Biol. *102*, 205–216.

Eng, J., Lynch, R.M., and Balaban, R.S. (1989). Nicotinamide adenine dinucleotide fluorescence spectroscopy and imaging of isolated cardiac myocytes. Biophys. J. *55*, 621–630.

Friedman, J.E., and Haddad, G.G. (1993). Major differences in $Ca^{2+}{}_{i}$ response to anoxia between neonatal and adult rat CA1 neurons: role of $Ca^{2+}{}_{o}$ and $Na^{+}{}_{o}$. J. Neurosci. *13*, 63–72.

Giroux, C., and Scatton, B. (1996). Ischemic stroke: treatment on the horizon. Eur. Neurol. *36*, 61–64.

Harteneck, C., Plant, T.D., and Schultz, G. (2000). From worm to man: three subfamilies of TRP channels. Trends Neurosci. *23*, 159–166.

Herson, P.S., Lee, K., Pinnock, R.D., Hughes, J., and Ashford, M.L. (1999). Hydrogen peroxide induces intracellular calcium overload by activation of a non-selective cation channel in an insulin-secreting cell line. J. Biol. Chem. *274*, 833–841.

Inoue, R., Okada, T., Onoue, H., Hara, Y., Shimizu, S., Naitoh, S., Ito, Y., and Mori, Y. (2001). The transient receptor potential protein homologue TRP6 is the essential component of vascular α_1-adrenoceptor-activated Ca^{2+}-permeable cation channel. Circ. Res. *88*, 325–332.

Kietzmann, T., Fandrey, J., and Acker, H. (2000). Oxygen radicals as messengers in oxygen-dependent gene expression. News Physiol. Sci. *15*, 202–208.

Klonowski-Stumpe, H., Schreiber, R., Grolik, M., Schulz, H., Häussinger, D., and Niederau, C. (1997). Effect of oxidative stress on cellular functions and cytosolic free calcium of rat pancreatic acinar cells. Am. J. Physiol. *272*, G1489–G1498.

Koliwad, S.K., Elliott, S.J., and Kunze, D.L. (1996). Oxidized glutathione mediates cation channel activation in calf vascular endothelial cells during oxidant stress. J. Physiol. *495*, 37–49.

Kourie, J.I. (1998). Interaction of reactive oxygen species with ion transport mechanisms. Am. J. Physiol. *275*, C1–C24.

Kuschel, L., Hansel, A., Schönherr, R., Weissbach, H., Brot, N., Hoshi, T., and Heinemann, S.H. (1999). Molecular cloning and functional expression of a human peptide methionine sulfoxide reductase (hMsrA). FEBS Lett. *456*, 17–21.

Li, A., Ségui, J., Heinemann, S.H., and Hoshi, T. (1998). Oxidation regulates cloned neuronal voltage-dependent Ca^{2+} channels expressed in *Xenopus* oocytes. J. Neurosci. *18*, 6740–6747.

Lin, S.J., Defossez, P.A., and Guarente, L. (2000). Requirement of NAD and *SIR2* for life-span extension by calorie restriction in *Saccharomyces cerevisiae.* Science *289*, 2126–2128.

Lipton, S.A., and Nicotera, P. (1998). Calcium, free radicals and excitotoxins in neuronal apoptosis. Cell Calcium *23*, 165–171.

Litt, M.R., Potter, J.J., Mezey, E., and Mitchell, M.C. (1989). Analysis of pyridine dinucleotides in cultured rat hepatocytes by high-performance liquid chromatography. Anal. Biochem. *179*, 34–36.

Maeno, E., Ishizaki, Y., Kanaseki, T., Hazama, A., and Okada, Y. (2000). Normotonic cell shrinkage because of disordered volume regulation is an early prerequisite to apoptosis. Proc. Natl. Acad. Sci. USA *97*, 9487–9492.

Mattson, M.P. (1996). Calcium and free radicals: mediators of neurotrophic factor and excitatory transmitter-regulated developmental plasticity and cell death. Perspect. Dev. Neurobiol. *3*, 79–91.

Mendez, F., and Penner, R. (1998). Near-visible ultraviolet light induces a novel ubiquitous calcium-permeable cation current in mammalian cell lines. J. Physiol. *507*, 365–377.

Nishida, M., Nagao, T., and Kurose, H. (1999). Activation of Rac1 increases c-jun NH_2-terminal kinase activity and DNA fragmentation in a calcium-dependent manner in rat myoblast cell line H9c2. Biochem. Biophys. Res. Commun. *262*, 350–354.

Okamoto, H. (1985). Molecular basis of experimental diabetes: degeneration oncogenesis and regeneration of pancreatic B-cells of islets of Langerhans. Bioessays *2*, 15–21.

Patel, A.J., Honoré, E., Maingret, F., Lesage, F., Fink, M., Duprat, F., and Lazdunski, M. (1998). A mammalian two pore domain mechanogated S-like K^{+} channel. EMBO J. *17*, 4283–4290.

Perraud, A.-L., Fleig, A., Dunn, C.A., Bagley, L.A., Launay, P., Schmitz, C., Stokes, A.J., Zhu, Q., Bessman, M.J., Penner, R., et al. (2001). ADP-ribose gating of the calcium-permeable LTRPC2 channel revealed by Nudix motif homology. Nature *411*, 595–599.

Ruppersberg, J.P., Stocker, M., Pongs, O., Heinemann, S.H., Frank, R., and Koenen, M. (1991). Regulation of fast inactivation of cloned mammalian I_K(A) channels by cysteine oxidation. Nature *352*, 711–714.

Sano, Y., Imamura, K., Miyake, A., Mochizuki, S., Yokoi, H., Matsushime, H., and Furuichi, K. (2001). Immunocyte Ca^{2+} influx system mediated by LTRPC2. Science *293*, 1327–1330.

Shimizu, S., Nomoto, M., Naito, S., Yamamoto, T., and Momose, K. (1998). Stimulation of nitric oxide synthase during oxidative endothelial cell injury. Biochem. Pharmacol. *55*, 77–83.

Tretter, L., and Adam-Vizi, V. (2000). Inhibition of Krebs cycle enzymes by hydrogen peroxide: a key role of α-ketoglutarate dehydrogenase in limiting NADH production under oxidative stress. J. Neurosci. *20*, 8972–8979.

Ueno, M., Masutani, H., Arai, R.J., Yamauchi, A., Hirota, K., Sakai, T., Inamoto, T., Yamaoka, Y., Yodoi, J., and Nikado, T. (1999). Thioredoxin-dependent redox regulation of p53-mediated p21 activation. J. Biol. Chem. *274*, 35809–35815.

Wink, D.A., Hanbauer, I., Krishna, M.C., DeGraff, W., Gamson, J., and Mitchell, J.B. (1993). Nitric oxide protects against cellular damage and cytotoxicity from reactive oxygen species. Proc. Natl. Acad. Sci. USA *90*, 9813–9817.

Xu, L., Eu, J.P., Meissner, G., and Stamler, J.S. (1998). Activation of the cardiac calcium release channel (ryanodine receptor) by poly-S-nitrosylation. Science *279*, 234–237.

Ziegler, M. (2000). New functions of a long-known molecule. Emerging roles of NAD in cellular signaling. Eur. J. Biochem. *267*, 1550–1564.